Mathematical modeling of the effects of nutrient competition and bile acid metabolism by the gut microbiota on colonization resistance against Clostridium difficile

Jabbari, Sara; Fleming-Davies, Arietta; Robertson, Suzanne L.; Asih, Tri Sri Noor; Lanzas, Cristina ; Lenhart, Suzanne ; Theriot, Casey M.

Chapter 1
Mathematical modeling of the effects of nutrient competition and bile acid metabolism by the gut microbiota on colonization resistance against *Clostridium difficile*

Arietta Fleming-Davies, Sara Jabbari, Suzanne L. Robertson, Tri Sri Noor Asih, Cristina Lanzas, Suzanne Lenhart, and Casey M. Theriot

Abstract *Clostridium difficile* is the leading cause of infectious diarrhea in hospitals and one of the most common healthcare associated infections. Antibiotics alter the normal gut microbiota and facilitate the colonization of enteric pathogens such as *C. difficile*. Our objective is to elucidate the role of bile acids and other mechanisms in providing colonization resistance against *C. difficile*. We formulated and analyzed differential equation models for microbial interactions in the gut and bile acid dynamics, as well as a combined model including both mechanisms. Our analysis indicates that bile acids do not prevent *C. difficile* colonization, but they regulate the onset of *C. difficile* colonization and growth after antibiotic perturbation. These results have implications in the development of novel ways to inhibit *C. difficile* infection.

Arietta Fleming-Davies
Department of Biology, Radford University e-mail: arietta.flemingdavies@gmail.com

Sara Jabbari
School of Mathematics, University of Birmingham e-mail: s.jabbari@bham.ac.uk

Suzanne L. Robertson
Department of Mathematics and Applied Mathematics, Virginia Commonwealth University e-mail: srobertson7@vcu.edu

Tri Sri Noor Asih
Department of Mathematics, Semarang State University e-mail: trisrinoorasih@gmail.com

Cristina Lanzas (correspondance)
Department of Population Health and Pathobiology, College of Veterinary Medicine, North Carolina State University e-mail: clanzas@ncsu.edu

Suzanne Lenhart (correspondance)
Department of Mathematics, University of Tennessee e-mail: lenhart@math.utk.edu

Casey M. Theriot (correspondance)
Department of Population Health and Pathobiology, College of Veterinary Medicine, North Carolina State University e-mail: cmtherio@ncsu.edu

Fleming-Davies, Jabbari, Robertson and Noor Asih contributed equally

1.1 Introduction

Clostridium difficile is an anaerobic, spore-forming, gram-positive bacillus first isolated in 1935 [11]. *C. difficile* is the leading cause of infectious diarrhea in hospitals. Symptoms associated with *C. difficile* infection (CDI) include diarrhea, abdominal pain and fever. In severe cases, CDI can cause colonic perforation, peritonitis, and death. CDI is a growing public health problem; in 2011, 453,000 primary infections, 83,000 first recurrences and 29,300 deaths were estimated in the United States alone [20].

Antibiotic therapy is a strong and independent risk factor for CDI [28, 30]. Antibiotics alter the indigenous gut microbiota decreasing colonization resistance against *C. difficile* [5, 32]. Colonization resistance is the ability of the indigenous gut microbiota to prevent colonization of enteric pathogens [43]. The gut microbiota provides colonization resistance against enteric pathogens in different ways, namely by competing for nutrients or space, producing bacteriocins or inhibitors, and stimulating the immune response [3, 31, 46]. Work from the past decade has started to shed light on how antibiotics lead to a loss of colonization resistance against *C. difficile*. Antibiotics alter the gut microbiota and metabolome; specifically, they affect the composition and concentration of bile acids, carbohydrates, and amino acids [2, 39, 40]. The gut microbiome and metabolic environment after antibiotics favors *C. difficile* spore germination and outgrowth.

C. difficile spores are resistant to denaturation and are metabolically dormant, allowing for transmission of the pathogen. Spores require specific bile acids for maximal germination into a metabolically active vegetative cell, where it requires amino acids and carbohydrates to grow to high cell density and produce toxins, which mediate disease [14, 36, 45]. The bile acid pool in the body consists of primary bile acids that are made by the host liver, which are further biotransformed into secondary bile acids by members of the gut microbiota [33]. Antibiotic alterations in the gut microbiota result in a loss of the microbial derived secondary bile acid deoxycholate (DCA), and an increase in the primary bile acid taurocholate (TCA), which enhances *C. difficile* spore germination and growth [39, 40]. Secondary bile acid DCA, which is present in the gut prior to antibiotic treatment, can inhibit the growth of *C. difficile* [36, 39]. Gut microbiota mediated secondary bile acids in the gut may play a role in colonization resistance against *C. difficile*.

Another possible mechanism of colonization resistance is competition for nutrients by members of the gut microbiota. Members of the gut microbiota have different metabolic requirements, and are able to compete for a variety of nutrients. *C. difficile* requires amino acids (cysteine, isoleucine, leucine, proline, tryptophan, and valine) and vitamins (biotin, pantothenate, and pyridoxine) for growth [6, 13]. In addition to these nutrients, *C. difficile* is also able to ferment carbohydrates including fructose, glucose, mannitol, mannose, melezitose, sorbitol, and sialic acids [25, 34]. Bacteria that overlap in metabolic requirements from the same *Clostridium* genus compete for similar nutrients *in vivo*, suppressing growth of pathogenic *C. difficile* [19, 24]. After antibiotic treatment there may be a decrease in bacteria that are able to compete against *C. difficile*, allowing the pathogen to grow uninhibited.

Several mechanistic models of colonization resistance have been developed and analyzed. Freter et al. [9] developed the first mathematical model of colonization resistance against *Escherichia coli* in the gastrointestinal tract. The model describes the population dynamics of two bacterial strains, the resident and invader. The two strains compete for nutrients and adhesion sites. The model is composed of four ordinary differential equations (ODEs) that track the overall resident strain population and the invader strain in three adhesion sites and uses the Monod functional form to model microbial growth. The model predicts that both strains can co-exist if the metabolically less efficient strain (invader) has specific adhesion sites for which it does not compete [9, 22]. Subsequent work expanded Freter's work to relax some of the underlying assumptions, such as perfect mixing or competition for a single nutrient [4, 8]. For example, Coleman et al. [8] developed a model with 11 ODEs that represent five carbon sources, five indigenous microbiota groups and one enteric pathogen, *Salmonella enterica*. Overall, the earlier models of colonization resistance considered different microbial groups depending on existent knowledge of the importance and interactions of each group and focused predominantly on nutrient competition.

In recent years, the availability of metagenomic high-throughput sequencing data has stimulated the development of data-driven models that reevaluate colonization resistance, particularly for *C. difficile*. Stein et al. [37] fitted a generalized Lotka-Volterra model to the abundance of the ten most abundant genera and *C. difficile* obtained from 16S rRNA high-throughput DNA sequencing data from a mouse model studying the effect of clindamycin on *C. difficile* colonization. A subset of four genera were identified as providing protection against *C. difficile*, but the underlying mechanisms were not modeled. Steinway et al. [38] used the same data to develop a Boolean dynamic model of the interactions among genera and used genome-scale metabolic reconstruction to gain insight into the mechanisms behind the interactions. No specific metabolic pathways were identified as an important source of the interactions between the gut microbiota and *C. difficile*. Despite using the same data, the studies differed on the bacterial genera that were deemed relevant to colonization resistance against *C. difficile*. Metagenomic 16S rRNA data is high-dimensional and sparse, and are reported as proportions, which may limit inference from the data [42]. Other mathematical models of *C. difficile* focus on disease transmission (e.g. [10, 17, 27]) or toxin production (e.g. [12]), but not colonization.

As the prevalance of antibiotic resistance rises, alternative treatment methods are being sought. Given the natural ability of the (undisturbed) gut microbiota to prevent *C. difficile* colonization, an obvious avenue for investigation is to consider how to recreate this natural defense mechanism in a compromised host. To achieve this, the factors involved must be better understood. In this paper, we use current knowledge of the mechanisms underlying interactions between key members of the gut microbiota and *C. difficile* to develop and analyze mathematical models that focus on colonization resistance. We use data from Theriot et al. [40] to model the contribution of bile acid metabolism and competition by members of the gut microbiota in both the pre-antibiotic treated gut, which is resistant to *C. difficile*, and the post-antibiotic treated gut, which is susceptible to *C. difficile*, to evaluate the

role of both mechanisms. Prior to antibiotic treatment the murine gut microbiota is dominated by two bacterial phyla, the Firmicutes (Lachnospiraceae family) and Bacteroidetes (Porphyromonadaceae family). After antibiotic treatment there is a shift in the murine gut microbiota to one that is dominated by members from the Firmicutes phylum (Lactobacillaceae family), where *C. difficile* is able to colonize. Similarly, prior to antibiotic treatment, the secondary bile acid DCA, which is an inhibitor of *C. difficile* growth, is present in the murine gut. After antibiotic treatment there is a loss of DCA and an increase in primary bile acid TCA in the gut, which *C. difficile* spores can utilize for germination and outgrowth. Members of the gut microbiota are important for the biotransformation of primary bile acids into secondary bile acids, TCA to cholate (CA) to DCA.

In Section 1.2 we formulate mathematical models for microbial interactions in the gut and bile acid dynamics, as well as a combined model including both mechanisms. Parameter estimation is discussed in Section 1.3, followed by an exploration of model dynamics in Section 1.4. We conclude with a discussion on the roles played by microbial interaction and bile acids in preventing *C. difficile* from colonizing the gut and how these could be manipulated for therapeutic benefit.

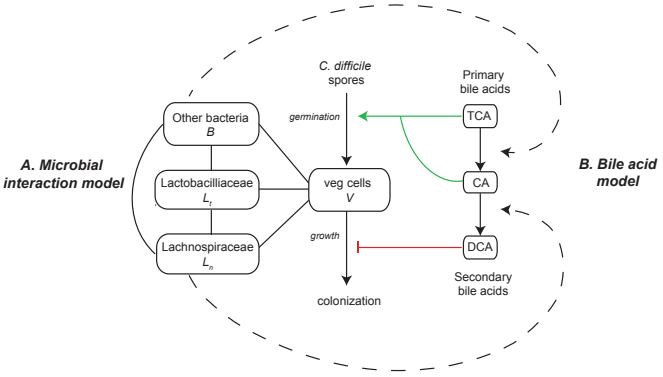

Fig. 1.1: Schematic of the models presented in this paper, representing the mechanisms of colonization resistance against *C. difficile* provided by the gut microbiota. A. Microbial interaction model between *C. difficile* vegetative cells, Lachnospiraceae, Lactobacillaceae, and other bacteria, which primarily compete with Lactobacilliaceae. B. Bile acid model showing the bacterial conversion from primary bile acid taurocholate (TCA) to cholate (CA) to secondary bile acid deoxycholate (DCA). The green lines represent positive interactions with *C. difficile* germination and growth and the red represent negative interactions. The dashed lines represent the combined model. Note that some Lactobacilliaceae members also have the ability to convert TCA to CA, which has been excluded from our model for simplicity.

1.2 Model development

To investigate the contributions of the two mechanisms described above to *C. difficile* colonization resistance, we analyze three ODE models: a model describing ecological interactions between groups of microbes in the gut, a model of the role of bile acid dynamics in *C. difficile* germination and outgrowth, and a combined model containing both mechanisms (see Figure 1.1). We analyze the dynamics of each of the three models separately. In all three models, we compare a pre-antibiotic gut to a post-antibiotic gut by changing the initial conditions. Antibiotics are not directly modeled; instead, initial conditions (presence of different microbial taxa) differ in the pre-antibiotic and post-antibiotic gut, depending on the susceptibility of the different microbial groups to antibiotics. As different antibiotics affect different species, we limit our assumptions to the antibiotic cefoperazone, in line with the data from Theriot et al. [40].

For simplicity, we have condensed the complex microbial community into four functional groups, based on their effects on *C. difficile* and bile acid production. The four groups modeled are:

1. *C. difficile* vegetative cells, V, which are susceptible to the antibiotic cefoperazone;
2. Firmicutes phylum (primarily from the Lachnospiraceae family), L_n, which convert the primary bile acid CA to the secondary bile acid DCA, are susceptible to the antibiotic cefoperazone, and are thought to compete directly with *C. difficile*;
3. Firmicutes phylum (primarily from the Lactobacilliaceae family), L_t, which do not affect bile acid metabolism, and are not susceptible to the antibiotic cefoperazone;
4. All other bacteria, B, which are dominated by the Bacteroidetes phylum (primarily from the Porphyromonadaceae family), are susceptible to the antibiotic cefoperazone, and are able to convert the bile acid TCA to CA.

See Table 1.1 for a summary of microbial taxa and traits. Note that there is evidence that DCA can also promote *C. difficile* germination, but at a much lower level than either TCA or CA [40, 47] and we accordingly omit this interaction term from the model.

Table 1.1: Summary of the four microbial groups considered in this study.

Microbial group	Susceptible to Cefoperazone?	Likely competitor for nutrients	Interactions with bile acids
C. difficile (V)	yes	L_n	DCA inhibits growth; CA and TCA promote germination
Lachnospiraceae (L_n)	yes	V	Converts CA to DCA
Lactobacilliaceae (L_t)	no	B	–
Other bacteria (B)	yes	L_t	Converts TCA to CA

1.2.1 Model of microbial interactions

We model interspecific interactions between each of the four microbial groups using a four-species Lotka-Volterra interaction model [29]:

$$\frac{dV}{dt} = r_V V(1 + \alpha_{VV}V + \alpha_{VL_n}L_n + \alpha_{VL_t}L_t + \alpha_{VB}B), \tag{1.1}$$

$$\frac{dL_n}{dt} = r_{L_n} L_n(1 + \alpha_{L_nV}V + \alpha_{L_nL_n}L_n + \alpha_{L_nL_t}L_t + \alpha_{L_nB}B), \tag{1.2}$$

$$\frac{dL_t}{dt} = r_{L_t} L_t(1 + \alpha_{L_tV}V + \alpha_{L_tL_n}L_n + \alpha_{L_tL_t}L_t + \alpha_{L_tB}B), \tag{1.3}$$

$$\frac{dB}{dt} = r_B B(1 + \alpha_{BV}V + \alpha_{BL_n}L_n + \alpha_{BL_t}L_t + \alpha_{BB}B). \tag{1.4}$$

Note that in our model, some interactions between groups are facilitative (positive) rather than competitive, and thus we refer to it as an "interaction" model rather than a competition model. Here V is the density of *C. difficile* vegetative cells, L_n is the density of Lachnospiraceae, L_t is the density of Lactobacillaceae, and B is the density of all other gut bacteria. Within-group and between-group interactions are described by the α terms, where α_{ij} gives the effect of group j on the growth rate of group i. Each α_{ij} may take a positive or negative value depending on whether group i has a net positive or negative effect on the other group (See Tables 1.2 and 1.6). Within-group competition is given by α_{ii}, the effect of group i on itself, and these values must always be negative. The intrinsic growth rate r_i is modified by the interaction of each group with all other groups, as $r_i(1 + \alpha_{iV}V + \alpha_{iL_n}L_n + \alpha_{iL_t}L_t + \alpha_{iB}B)$. See Table 1.3 for initial conditions in the pre-antibiotic and post-antibiotic gut and Table 1.6 for the default parameter set.

Table 1.2: Signs of interaction coefficients for the microbial interaction and full models. The sign of each α_{ij}, indicating the effect of microbial group j on microbial group i, is found in cell i, j of the table. Negative values indicate a competitive effect, while positive values indicate a facilitative effect. Note that for some groups, α_{ij} is very close to zero (see Table 1.6 for exact values). These were estimated from limited data and may be subject to change.

	V	L_n	L_t	B
V	-	-	+	-
L_n	+	-	+	-
L_t	+	-	-	-
B	+	+	+	-

Table 1.3: Initial conditions for numerical simulations of the microbial interactions model in the pre-antibiotic and post-antibiotic gut. Note that in the pre-antibiotic gut we have unrealistically high levels of *C. difficile* and Lactobacilliaceae to illustrate how a "healthy" gut could evolve purely from microbial interactions. In the post-antibiotic simulations, we assume all Lachnospiraceae and other bacteria are wiped out and a small number of *C. difficile* and Lactobacilliaceae are introduced. The stability conditions of this model (discussed in Section 1.4.1) mean that the initial conditions in each case can be very broad to achieve the same steady states.

Scenario	Term	Definition	Value
Pre-antibiotics	$V(0)$	*C. difficile* vegetative cells	1×10^8
	$L_n(0)$	Lachnospiraceae	1×10^8
	$L_t(0)$	Lactobacilliaceae	1×10^8
	$B(0)$	Other bacteria	1×10^8
Post-antibiotics	$V(0)$	*C. difficile* vegetative cells	100
	$L_n(0)$	Lachnospiraceae	0
	$L_t(0)$	Lactobacilliaceae	100
	$B(0)$	Other bacteria	0

1.2.2 Model of bile acid interactions

Here we model a simplified system of the production and conversion of three key bile acids that interact with *C. difficile* vegetative cells, V, and *C. difficile* spores, S:

$$\frac{dV}{dt} = g(T+C)S + \frac{r_V}{1+bD^2}(1+\alpha_{VV}V)V, \tag{1.5}$$

$$\frac{dT}{dt} = h - \delta_T T - \frac{v_T BT}{M_T+T}, \tag{1.6}$$

$$\frac{dC}{dt} = \frac{v_T BT}{M_T+T} - \delta_C C - \frac{v_C L_n C}{M_C+C}, \tag{1.7}$$

$$\frac{dD}{dt} = \frac{v_C L_n C}{M_C+C} - \delta_D D, \tag{1.8}$$

$$\frac{dS}{dt} = -g(T+C)S. \tag{1.9}$$

T, C, and D represent the bile acids TCA, CA, and DCA, respectively. In the model of bile acid dynamics alone, vegetative *C. difficile* cells are the only one of the four microbial groups explicitly modeled (eq. 1.5). Spores germinate at a rate $g(T+C)$, which is an increasing function of the bile acids TCA and CA. Growth of vegetative cells of *C. difficile* is modeled as in the microbial interactions model (eq. 1.1), but including only intraspecific competition. In this model, however, the growth rate of *C. difficile* vegetative cells is a decreasing function of the concentration of the bile acid DCA.

The conversion between different bile acids (TCA to CA and CA to DCA) are modeled using the Michaelis-Menten kinetics function, where the reaction rate depends on the concentrations of the substrate and product. The parameters M_T and M_C are the half saturation values, the substrate concentrations at which the corresponding reaction rates are half of the maximum corresponding reaction rates given by v_T and v_C, respectively. Lachnospiraceae, L_n, convert the bile acid CA to the bile acid DCA (eq. 1.7), and other bacteria, B, convert the bile acid TCA to the bile acid CA (eq. 1.6). In the bile acid model, L_n and B population sizes are held constant and not explicitly modeled. All bile acids are subject to natural degradation and a source term for TCA is included. See Table 1.4 for initial conditions in the pre-antibiotic and post-antibiotic gut.

Table 1.4: Initial conditions for numerical simulations of the bile acid model in the pre-antibiotic and post-antibiotic gut. In the pre-antibiotic gut the values of L_n and B are taken to be their steady states in the pre-antibiotic simulation of the microbial interaction model. The initial condition of DCA is chosen to be relevant to *C. difficile*-growth-inhibiting concentrations. The initial number of spores is chosen to match experimental work, e.g. [16].

Scenario	Term	Definition	Value
Pre-antibiotics	$V(0)$	*C. difficile* vegetative cells	0
	L_n	Lachnospiraceae (assumed constant)	9.867×10^7
	B	Other bacteria (assumed constant)	1.3305×10^8
	$T(0)$	Concentration of TCA	4×10^{-4}
	$C(0)$	Concentration of CA	5×10^{-3}
	$D(0)$	Concentration of DCA	0.1
	$S(0)$	*C. difficile* spores	100
Post-antibiotics	$V(0)$	*C. difficile* vegetative cells	0
	L_n	Lachnospiraceae (assumed constant)	0
	B	Other bacteria (assumed constant)	0
	$T(0)$	Concentration of TCA	4×10^{-4}
	$C(0)$	Concentration of CA	5×10^{-3}
	$D(0)$	Concentration of DCA	0.1
	$S(0)$	*C. difficile* spores	100

1.2.3 Combined model

In the combined model, growth of vegetative *C. difficile* cells, V, is modified by interactions with other microbial taxa as well as by the concentration of the bile acid DCA present in the gut:

$$\frac{dV}{dt} = \frac{r_V V}{1+bD^2}(1+\alpha_{VV}V+\alpha_{VL_n}L_n+\alpha_{VL_t}L_t+\alpha_{VB}B)+g(T+C)S, \quad (1.10)$$

$$\frac{dL_n}{dt} = r_{L_n}L_n(1+\alpha_{L_nV}V+\alpha_{L_nL_n}L_n+\alpha_{L_nL_t}L_t+\alpha_{L_nB}B), \quad (1.11)$$

$$\frac{dL_t}{dt} = r_{L_t}L_t(1+\alpha_{L_tV}V+\alpha_{L_tL_n}L_n+\alpha_{L_tL_t}L_t+\alpha_{L_tB}B), \quad (1.12)$$

$$\frac{dB}{dt} = r_B B(1+\alpha_{BV}V+\alpha_{BL_n}L_n+\alpha_{BL_t}L_t+\alpha_{BB}B), \quad (1.13)$$

$$\frac{dT}{dt} = h-\delta_T T-\frac{v_T BT}{M_T+T}, \quad (1.14)$$

$$\frac{dC}{dt} = \frac{v_T BT}{M_T+T}-\delta_C C-\frac{v_C L_n C}{M_C+C}, \quad (1.15)$$

$$\frac{dD}{dt} = \frac{v_C L_n C}{M_C+C}-\delta_D D, \quad (1.16)$$

$$\frac{dS}{dt} = -g(T+C)S. \quad (1.17)$$

As in the bile acid model, Lachnospiraceae bacteria, L_n, convert the bile acid CA to the bile acid DCA, and other bacteria, B, convert the bile acid TCA to the bile acid CA. However, here the populations of L_n and B are explicitly modeled (eqs.1.11 and 1.13, respectively), with growth rates affected by each group's interactions with other microbes as in the microbial interaction model. See Table 1.5 for initial conditions in the pre-antibiotic and post-antibiotic gut and Table 1.6 for the default parameter set.

1.3 Parameter estimation

We currently have insufficient data to reliably estimate the relatively high number of model parameters. Furthermore, since we are collating many different microbial taxa within each group, it would be unwise to speculate on the exact value of the parameters. Instead we have used available data as follows to gauge initial estimates where possible and focus on qualitative, rather than quantitative conclusions from the model simulations. In addition, we performed sensitivity analysis for the uncertain parameters.

Growth curves for *C. difficile* in brain heart infusion (BHI) media supplemented with different concentrations of DCA [39], Lachnospiraceae in minimal media (unpublished data) and Lactobacilliaceae in MRS media [26] were used to estimate the growth rates r_V, r_{L_n}, and r_{L_t} by fitting a logistic function to the data up to the points where the growth curves exhibited logistic growth. Optical density (OD) measurements were scaled by 2×10^8 to account for the conversion from OD to cell number. Data of *C. difficile* in BHI media were used to estimate growth rates under different concentrations of DCA (Figure 1.2a, for example); we then fit a nonlinear function of the form $a/(1+bD^2)$ (Figure 1.2b) to create a function that represents inhibi-

Table 1.5: Initial conditions for numerical simulations of the combined model in the pre-antibiotic and post-antibiotic gut. In both cases we start with a small number of *C. difficile* spores. In the pre-antibiotic case we start with equal L_t, L_n and B to see how the latter two outcompete L_t and V. In the post-antibiotic case we assume both L_n and B are wiped out and L_t is introduced to the system.

Scenario	Term	Definition	Value
Pre-antibiotics	$V(0)$	*C. difficile* vegetative cells	0
	$L_n(0)$	Lachnospiraceae	1×10^8
	$L_t(0)$	Lactobacilliaceae	1×10^8
	$B(0)$	Other bacteria	1×10^8
	$T(0)$	Concentration of TCA	4×10^{-4}
	$C(0)$	Concentration of CA	5×10^{-3}
	$D(0)$	Concentration of DCA	0.1
	$S(0)$	*C. difficile* spores	100
Post-antibiotics	$V(0)$	*C. difficile* vegetative cells	0
	$L_n(0)$	Lachnospiraceae	0
	$L_t(0)$	Lactobacilliaceae	1
	$B(0)$	Other bacteria	0
	$T(0)$	Concentration of TCA	4×10^{-4}
	$C(0)$	Concentration of CA	5×10^{-3}
	$D(0)$	Concentration of DCA	0.1
	$S(0)$	*C. difficile* spores	100

tion of *C. difficile* growth by DCA. However, since Lachnospiraceae are believed to be the main competitors for nutrients with *C. difficile* and our growth rate for the Lachnospiraceae was estimated from data extracted from minimal media, this function was scaled so that in the absence of DCA it would equal the growth rate of *C. difficile* estimated from another data set for *C. difficile* measured in minimal media. Since the other bacterial group represents a collection of bacteria, we simply used the same growth rate as that for the Lactobacilliaceae as they use similar resources (Table 1.1).

All microbial interaction coefficients α_{ij} were summarized from data from Stein et al. [37]. In order to simplify microbial interactions into just 4 groups, we summed the terms α_{ij} from Stein et al. across all taxa within each of our 4 groups. Interaction coefficients α_{ij} ranged from negative (competition) to positive (facilitation). We chose not to specify signs of the interaction coefficients in the model equations, as these depend on parameter values and are not based on known mechanisms of ecological interactions between groups. The signs of the interaction coefficients (and thus the direction of the effects) are summarized in Table 1.2.

In order for each group of bacteria to be able to achieve steady states of the correct order of magnitude (based on the growth curves mentioned above) when simulated in isolation from the other species, the α_{ij} were each scaled by 2×10^{-8} to maintain relative sizes and then rounded to one decimal place (notice that carrying

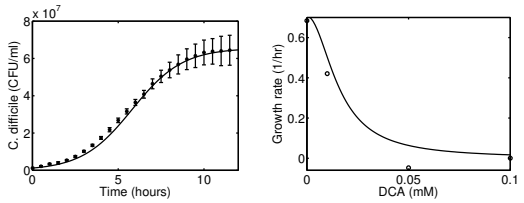

(a) (b)

Fig. 1.2: (a) Logistic growth fit (solid line) to *in vitro C. difficile* growth data in BHI media with no DCA (asterisks) [39] (estimated growth rate for this example 0.6839 h^{-1}, and carrying capacity 6.554×10^7). Error bars signify standard deviation from the mean (from 3 repeats). (b) Estimated *in vitro* growth rates of *C. difficile* at different concentrations of the bile acid DCA (circles) were used to fit a function of the form $a/(1+bD^2)$ describing the inhibition of *C. difficile* vegetative growth by DCA (solid line). Data from Theriot et. al [39]

capacities are not included explicitly in the model). For the model to reproduce what is seen in experimental work [40] (B and L_n dominating the pre-antibiotic gut and L_t dominating initially in a post-antibiotic gut), three of the α_{ij} were subsequently modified ($\alpha_{LnB}, \alpha_{LtV}$ and α_{LtB}), but kept within the range of the other α_{ij} and their positive or negative effects maintained.

Enzyme kinetics parameters for CA and DCA production were chosen to produce reasonable concentrations of TCA, CA, and DCA at steady state [33].

The default parameter set is used throughout the paper unless otherwise stated and can be found in Table 1.6.

1.4 Model dynamics

1.4.1 Microbial interaction model dynamics

Figure 1.3a depicts the pre-antibiotic gut simulation for the microbial interaction model (eqs. 1.1–1.4) and shows how the interactions between the different groups of microbes can determine the make-up of the gut. *C. difficile* and Lactobacillaceae cells are quickly forced to zero steady states by the growth of Lachnospiraceae and the other bacteria, in agreement with [5, 39], where the dominant bacteria in a gut that has not been exposed to antibiotics fall largely into these two groups.

It can be shown mathematically that this steady state (where $V = L_t = 0$ but L_n and B co-exist) is locally stable under our parameter regime. To simulate the post-antibiotic gut, where antibiotics are assumed to kill the Lachnospiraceae and other bacteria, we must remove these two groups from the system entirely to avoid returning to the pre-antibiotic steady state. Setting $B(0) = L_n(0) = 0$ and assuming small

Table 1.6: Parameter values for the combined model, including both the microbial interaction model (top section) and the bile acid model (lower section). All interaction coefficients α_{ij} are summarized from data from Stein et al. [37]. Growth rates were fit to *in vitro* experimental data from Theriot et al. [39]. Enzyme kinetics parameters for CA and DCA production were chosen to produce reasonable concentrations of TCA, CA, and DCA at the steady state [33]

Parameter	Definition	Units	Value
r_V	Growth rate of *C. difficile* vegetative cells	h^{-1}	0.332
r_{L_n}	Growth rate of Lachnos	h^{-1}	0.711
r_{L_t}	Growth rate of Lactos	h^{-1}	0.665
r_B	Growth rate of other bacteria	h^{-1}	0.665
α_{VV}	Effect of V on V	cells^{-1} h^{-1}	-3×10^{-9}
α_{VL_n}	Effect of L_n on V	cells^{-1} h^{-1}	-6×10^{-9}
α_{VL_t}	Effect of L_t on V	cells^{-1} h^{-1}	1×10^{-9}
α_{VB}	Effect of B on V	cells^{-1} h^{-1}	-6×10^{-9}
α_{L_nV}	Effect of V on L_n	cells^{-1} h^{-1}	8×10^{-9}
$\alpha_{L_nL_n}$	Effect of L_n on L_n	cells^{-1} h^{-1}	-1×10^{-8}
$\alpha_{L_nL_t}$	Effect of L_t on L_n	cells^{-1} h^{-1}	8×10^{-10}
α_{L_nB}	Effect of B on L_n	cells^{-1} h^{-1}	-1×10^{-10}
α_{L_tV}	Effect of V on L_t	cells^{-1} h^{-1}	2×10^{-10}
$\alpha_{L_tL_n}$	Effect of L_n on L_t	cells^{-1} h^{-1}	-8×10^{-10}
$\alpha_{L_tL_t}$	Effect of L_t on L_t	cells^{-1} h^{-1}	-5×10^{-9}
α_{L_tB}	Effect of B on L_t	cells^{-1} h^{-1}	-1×10^{-8}
α_{BV}	Effect of V on B	cells^{-1} h^{-1}	8×10^{-9}
α_{BL_n}	Effect of L_n on B	cells^{-1} h^{-1}	2×10^{-9}
α_{BL_t}	Effect of L_t on B	cells^{-1} h^{-1}	9×10^{-10}
α_{BB}	Effect of B on B	cells^{-1} h^{-1}	-9×10^{-9}
b	Inhibition of *C. difficile* growth by DCA	mM^{-2}	4037
h	Production of TCA	mM h^{-1}	0.01
g	Germination rate of *C. difficile* spores	h^{-1} mM^{-1}	10
v_T	Production of CA from TCA	mM cells^{-1} h^{-1}	4×10^{-8}
v_C	Production of DCA from CA	mM cells^{-1} h^{-1}	4×10^{-8}
M_T	Half saturation of CA production	mM	0.6325
M_C	Half saturation of DCA production	mM	0.6325
δ_T	TCA decay rate	h^{-1}	0.1
δ_C	CA decay rate	h^{-1}	0.1
δ_D	DCA decay rate	h^{-1}	0.1

numbers of V and L_t are present (Figure 1.3b) enables the Lactobacillaceae and *C. difficile* to coexist. Lactobacillaceae dominates initially, but *C. difficile* eventually grows to higher numbers, reaching levels where it could likely establish colonization in the gut. Other bacteria inhibit the three remaining groups (see Table 1.2). The Lachnospiraceae also inhibit all groups apart from other bacteria, which they pro-

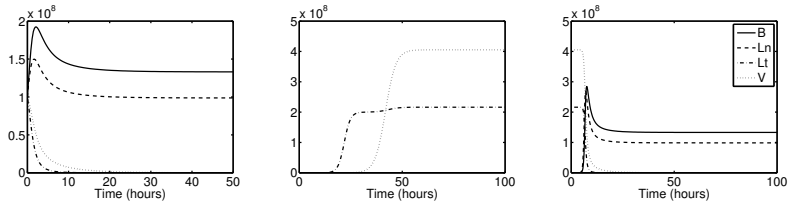

(a) (b) (c)

Fig. 1.3: Numerical solutions to the microbial interaction model (eqs. 1.1-1.4). In (a) all four groups begin at equal concentrations and the interactions between the groups force V and L_t into zero steady states. Removing L_n and B in (b) enables *C. difficile* to establish colonization. Using the steady states of V and L_t from (b) as initial conditions in (c), and re-introducing L_n and B through $L_n(0) = B(0) = 1$ results in restoration of the pre-antibiotic gut microbiota.

mote, hence reinforcing the dominance of other bacteria when present. Therefore, removing these two groups essentially gives *C. difficile* and the Lactobacillaceae the freedom to grow. The Lactobacillaceae have a higher growth rate, so they emerge initially. Both *C. difficile* and the Lactobacillaceae promote each other's growth, but the Lactobacillaceae do this more strongly in our parameter set ($\alpha_{VL_t} > \alpha_{L_tV}$), hence *C. difficile* will eventually take over and dominate the gut, i.e. though the Lactobacillaceae have a higher growth rate than *C. difficile*, the *C. difficile* bacteria can be considered to have a higher relative fitness under our parameter set. This replicates the microbiome dynamics detected in [40] well.

In the absence of L_n and B, the model of microbial interactions is reduced to a two dimensional system with equations for V and L_t. For the V, L_t system, the co-existence equilibrium is locally stable [29] if

$$\frac{\alpha_{VL_t}\alpha_{L_tV}}{\alpha_{VV}\alpha_{L_tL_t}} < 1.$$

The condition holds when intragroup competition dominates over the V, L_t cooperative interaction; in this simple system with our parameter values, in the numerator α_{VL_t} and α_{L_tV} are both positive while in the denominator, α_{VV} and $\alpha_{L_tL_t}$ are both negative. When considering the full microbial interactions model with 4 equations, it is interesting to note that the equilibrium with $L_n = B = 0$ and V and L_t positive is unstable. Thus re-introducing B and L_n into the model following *C. difficile* colonization enables fast restoration of the gut to the pre-antibiotic stable steady state (Figure 1.3c). We note that in reality this would be unlikely to occur, at least on this timescale, due to the host of post-colonization mechanisms employed by *C. difficile* to establish infection that are not included in this model. Interestingly, re-introducing either B or L_n without the other is not sufficient to restore the gut to eradicate the *C. difficile* cells (Figure 1.4). We note that these results are highly de-

pendent on the values of the interaction parameters and require further investigation once more data is available for parameterization of the model.

Using our parameters, we investigated all the feasible equilibria (non-negative components) for this system. Besides the two cases mentioned above, note that there are also three other feasible, unstable equilibria with two components being zero: $L_n = L_t = 0, B = V = 0, B = L_t = 0$, i.e. other bacteria and *C. difficile* cells can co-exist, as can Lachnospiraceae and Lactobacillaceae or *C. difficile* and Lachnospiraceae. There is one feasible equilibrium with only one zero component: when $B = 0$, there is an unstable equilibrium with the other three taxa able to survive together. Equilibria with three zero components are not relevant here since they only tell us that each of the microbial taxa can survive in isolation. Interestingly, there is not a feasible equilibrium with four positive components: under our parameter choice at least one microbial group will not be able to survive in the presence of the others, matching what is seen in mouse models of *C. difficile* infection, e.g. [16, 40]. The full stability analysis therefore tells us that the only feasible and stable steady state is that where other bacteria and Lachnospiraceae co-exist while suppressing *C. difficile* and the Lactobacillaceae.

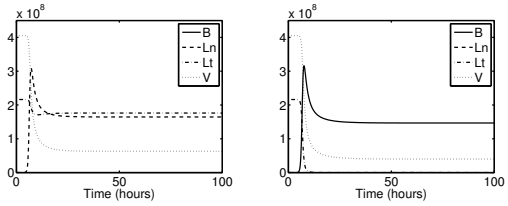

(a) (b)

Fig. 1.4: The microbial interaction model with $V(0)$ and $L_t(0)$ taken to be the steady states of Figure 1.3b and (a) $L_n(0) = 1, B(0) = 0$ (b) $L_n(0) = 0, B(0) = 1$. In either of these scenarios co-existence with *C. difficile* can occur.

1.4.2 Bile acid model dynamics

Considering the effect of metabolites on *C. difficile* in isolation enables us to track the effect of bile acids on the germination of spores and outgrowth of vegetative *C. difficile* cells. Solving eqs. 1.5–1.9 numerically in Figure 1.5 allows us to compare the pre-antibiotic gut microbiota (where B and L_n are present and can catalyze the conversion of TCA to CA and CA to DCA, respectively) to the post-antibiotic gut microbiota metabolism where neither B or L_n are present. Spore germination, triggered largely by TCA, occurs much faster in the post-antibiotic model but outgrowth of vegetative cells does occur in both cases. Indeed, V reaches the same steady state under both conditions, but in the pre-antibiotic case (Figure 1.5, solid line) this level

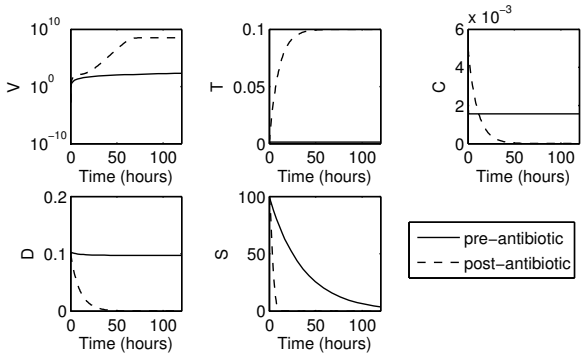

Fig. 1.5: Numerical simulations to the bile acid model (eqs. 1.5–1.9) in the pre-antibiotic regime (B and L_n taken to be the steady states of the pre-antibiotic microbial interaction model, solid line) and post-antibiotic ($B = L_n = 0$, dashed line). Note that V is plotted on a log-scale for clarity. Initial conditions are taken from Table 1.4.

is attained over the unrealistic timescale of 2000 hours (simulation not illustrated over that timescale). Over the five days simulated, while vegetative *C. difficile* cells are present in the pre-antibiotic model, they don't reach what might be deemed significant levels for colonization. Conversely, in the post-antibiotic model (Figure 1.5, dashed line) these levels are reached within four days (which is a feasible timeframe). Bile acids alone, therefore, cannot represent the full long-term mechanisms of colonization resistance in the pre-antibiotic state. Another factor, whether that is microbial interactions or the immune response, say, must also play a part. However, given that experimental evidence does suggest that bile acids are involved in protecting the gut from colonization (e.g. through inhibition of *C. difficile* growth [36, 39]), we can explore the model further to elucidate this role.

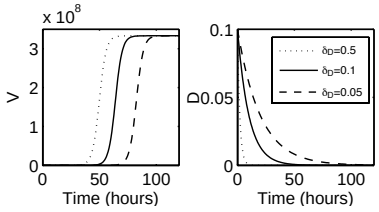

Fig. 1.6: Numerical solutions to the bile acid model under post-antibiotic conditions ($B = L_n = 0$) and varying the degradation rate of DCA, δ_D (default value is $\delta_D = 0.1$). Lowering the value of δ_D delays the onset of colonization.

The sensitivity analysis in Section 1.4.2.1 below suggests further investigation into the degradation rate of DCA, δ_D. At sufficiently high levels, DCA inhibits

growth of *C. difficile* (Figure 1.2b). Therefore, the rate at which it degrades out of the system once antibiotics have cleared the gut of Lachnospiraceae bacteria, preventing more DCA from being produced, will be instrumental in determining vegetative *C. difficile* dynamics. Since DCA will always eventually degrade out of the system in the absence of Lachnospiraceae, δ_D does not affect final *C. difficile* numbers; however, the timing of the onset of colonization is affected, occurring earlier with faster degradation of DCA (see Figure 1.6). This model therefore suggests that bile acids may be more important in delaying colonization than in ultimately preventing it. Of course, we must consider that there are likely to be additional factors besides those included in this model that could also affect DCA levels over time.

1.4.2.1 Sensitivity analysis on bile acid model

To assess the effect of specific bile acid model parameters on *C. difficile* dynamics, we performed a sensitivity analysis on the model following [21] with a model output of maximum *C. difficile* vegetative cells after either 6 hours, 48 hours, or 120 hours. Model parameters were varied uniformly over the ranges shown in Table 1.7 using Latin Hypercube Sampling. Methods and code from [15] and [21] were used to calculate partial rank correlation coefficients (PRCCs). PRCC values and their corresponding p-values are reported in Table 1.7.

After 6 hours, maximum *C. difficile* levels are most sensitive to the decay rate of DCA (δ_D, see Figure 1.6), the intrinsic growth rate of *C. difficile* (r_V), and the coefficient b, which determines the strength of inhibition of the growth rate of *C. difficile* by DCA. Although the PRCCs for g, h, and α_{VV} are also statistically significant ($p < 0.0001$), their values are low indicating they do not have a large effect on maximum *C. difficile* levels.

As time since introduction of spores increases, maximum *C. difficile* levels become more sensitive to α_{VV} and less sensitive to r_V and δ_D. By 120 hours, *C. difficile* cells have either reached or grown close to carrying capacity. At this time maximum *C. difficile* levels are most sensitive to α_{VV} and r_V, parameters that determine the value of this carrying capacity. The PRCC for δ_D is still significant but decreases from 0.8858 to 0.1138. This is not surprising as the decay rate of DCA has a large effect on the rate of growth of *C. difficile*, affecting when carrying capacity is reached but not the value of the carrying capacity itself (Figure 1.6).

1.4.3 Combined model dynamics

Figure 1.7 depicts the numerical solution to the combined microbial interaction and bile acid model, i.e. eqs. 1.10–1.17. We see the results of the microbial interaction model reproduced in the sense that for the pre-antibiotic case Lachnospiraceae and other bacteria co-exist, with the situation reversed in the post-antibiotic model. The system achieves near identical steady states to the microbial interaction model and

Table 1.7: Partial Rank Correlation Coefficient (PRCC) and p-values from a global sensitivity analysis of the bile acid model with $N = 5,000$ (number of model runs). Output is maximum *C. difficile* vegetative cells after 6 hours, 48 hours, and 120 hours. Statistically significant PRCCs ($p < 0.0001$) are bolded.

Parameter	Range	After 6 hours		After 48 hours		After 120 hours	
		PRCC	p-value	PRCC	p-value	PRCC	p-value
δ_D	$(10^{-4}, 1)$	$\mathbf{0.8858}$	< 0.0001	$\mathbf{0.3326}$	< 0.0001	$\mathbf{0.1138}$	< 0.0001
r_V	$(0.1, 1)$	$\mathbf{0.8407}$	< 0.0001	$\mathbf{0.7576}$	< 0.0001	$\mathbf{0.4986}$	< 0.0001
b	$(10^3, 10^4)$	$\mathbf{-0.4280}$	< 0.0001	-0.0244	0.0854	-0.0141	0.3185
g	$(0.1, 100)$	$\mathbf{0.1031}$	< 0.0001	0.0034	0.8077	-0.0180	0.2035
h	$(10^{-4}, 1)$	$\mathbf{0.0853}$	< 0.0001	0.0080	0.5708	-0.0196	0.1656
α_{VV}	$(-10^{-8}, -10^{-10})$	$\mathbf{0.0305}$	< 0.0001	$\mathbf{0.5127}$	< 0.0001	$\mathbf{0.7979}$	< 0.0001
v_C	$(10^{-10}, 0.1)$	0.0189	0.1812	0.0070	0.6216	-0.0108	0.4471
δ_T	$(10^{-4}, 1)$	-0.0169	0.2316	-0.0172	0.2236	0.0149	0.2913
Ln	$(0, 10^{10})$	-0.0163	0.2485	-0.0089	0.5288	-0.0049	0.7300
M_T	$(0.01, 1)$	0.0157	0.2678	0.0010	0.9421	-0.0129	0.3626
B	$(0, 10^{10})$	$-.0142$	0.3159	0.0168	0.2370	0.0241	0.0885
v_T	$(10^{-10}, 0.1)$	-0.0125	0.3786	-0.0007	0.9609	0.0099	0.4837
M_C	$(0.01, 1)$	0.0109	0.4405	0.0152	0.2828	0.0017	0.9070
δ_C	$(10^{-4}, 1)$	0.0104	0.4644	-0.0003	0.9834	0.0125	0.3770

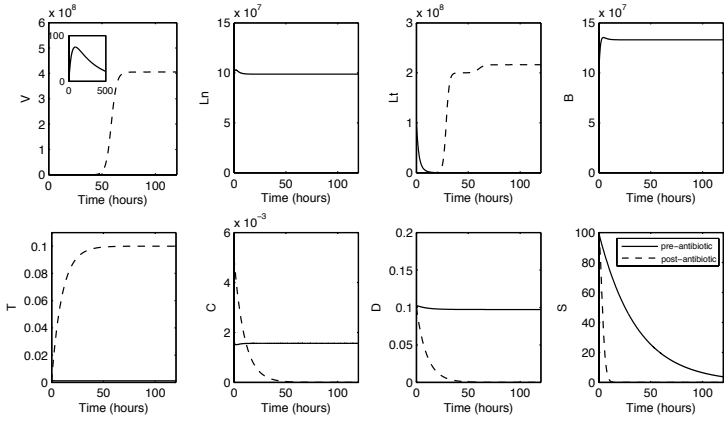

Fig. 1.7: Numerical solution to the combined model (eqs. 1.10–1.17) for the pre- (solid line) and post-antibiotic (dashed line) conditions. In the first panel we use an inset to illustrate that spores do germinate to cause a rise in *C. difficile* vegetative cells, but microbial competition quickly suppresses these so that this is not visible on the outer figure. In the post-antibiotic simulation, both L_n and B are zero throughout the timecourse.

here we are not seeing the role for bile acids in the loss of colonization resistance in the post-antibiotic simulation. However, drawing on our investigations in Section

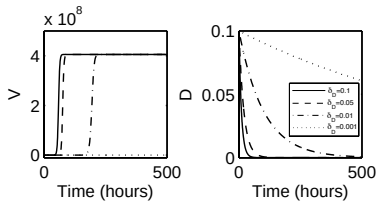

Fig. 1.8: Numerical solution to the combined model under a range of values of δ_D and the post-antibiotic conditions. The slower DCA degrades, the longer colonization can be prevented.

1.4.2, we simulate the combined model with varying values of δ_D, the degradation rate of DCA (Figure 1.8), and again see that this secondary bile acid may play a crucial role in the onset of colonization in the post-antibiotic case. Thus it is possible that each of the two colonization-resistance mechanisms we have modeled have their own purpose: following disruption of the microbiome by antibiotics, bile acids could effectively delay the onset of colonization, providing a window of opportunity for microbial competition to restore the flora to a *C. difficile*-resistant state. We demonstrate this in Figure 1.9. Note that, as in the microbial interaction model, restoration would occur even if B and L_n are re-introduced when V is at colonization-indicative levels because we have not included any post-colonization mechanisms in the current model formulation that could prevent this occurring. Nevertheless, we include this simulation for illustrative purposes. As in the microbial interaction model, *both* L_n and B must be introduced to restore the gut, i.e. neither one can achieve this in isolation.

A possible therapy to prevent *C. difficile* infection therefore could be to manipulate DCA production by maintaining it in a sufficiently high state to delay the onset of colonization for long enough for the pre-antibiotic flora to restore itself.

1.4.3.1 Sensitivity analysis on combined model

To assess the effect of the parameters in the combined model, we again performed a global sensitivity analysis with a model output of maximum *C. difficile* vegetative cells. We looked at this output at 6, 48 and 120 hours after the introduction of *C. difficile* spores into a post-antibiotic gut, using the initial conditions in Table 1.5. Parameter ranges, PRCCs and corresponding p-values can be found in Table 1.8. The interaction coefficients α_{ij} were held constant at their values in Table 1.6 and were not included in the sensitivity analysis.

We find that after 6 hours, maximum *C. difficile* vegetative cells are most sensitive to the same five parameters as in the bile acid model (δ_D, r_V, b, g, and h),

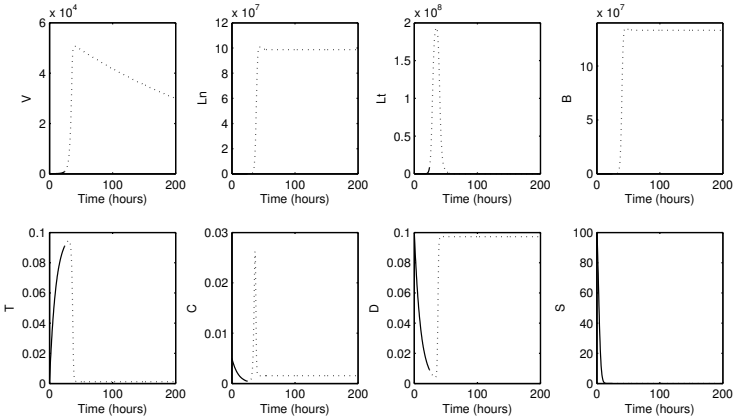

Fig. 1.9: Numerical simulation of the combined model under post-antibiotic conditions (i.e. $B(0) = L_n(0) = 0$) but where B and L_n are re-introduced to the gut at time $t = 24$ (i.e. $B(24) = L_n(24) = 1000$ – values chosen for illustrative purposes, lower numbers would achieve equivalent results in the long term). The addition of microbial interactions enables the gut to inhibit *C. difficile* vegetative cell growth sufficiently to prevent colonization and eradicate the pathogen from the gut (over a longer timescale than shown here). Solid lines are used to illustrate $t \leq 24$ and dotted for $t > 24$.

with PRCCs of similar magnitude. After 48 hours, the growth rate of *C. difficile* vegetative cells (r_V) still has the highest PRCC. However, the next highest PRCC is the growth rate of Lactobacillaceae (r_{Lt}). Increasing r_{Lt} allows Lactobacillaceae to grow to high levels more quickly, where they are able to have a positive impact on the growth of *C. difficile* vegetative cells (since $\alpha_{VLt} > 0$). Sensitivity to the growth rate of Lactobacillaceae increases with time since introduction of *C. difficile* spores, and at 120 hours r_{LT} has the highest PRCC.

1.5 Discussion

Earlier models of colonization resistance explicitly addressed two mechanisms: competition for a single nutrient and competition for adhesion sites [9]. Recent research has identified numerous mechanisms by which resident gut microbiota can inhibit pathogens including: 1) competition for nutrients, 2) indirect inhibition mediated by the host immune system, 3) metabolic exclusion by short chain fatty acids, 4) direct inhibition by bacteriocins, and 5) inhibition by bile acids [18, 41]. In particular, bile acids interact with *C. difficile* in a complex way. In our paper, we model the interactions between bile acids and *C. difficile* explicitly, whereas we model

Table 1.8: Partial Rank Correlation Coefficient (PRCC) and p-values from a global sensitivity analysis of combined model under post-antibiotic conditions with N = 5,000 (number of model runs). Output is maximum *C. difficile* vegetative cells after 6 hours, 48 hours, and 120 hours. Statistically significant PRCCs ($p < 0.0001$) are bolded.

Parameter	Range	After 6 hours		After 48 hours		After 120 hours	
		PRCC	p-value	PRCC	p-value	PRCC	p-value
δ_D	$(10^{-4}, 1)$	$\mathbf{0.9252}$	< 0.0001	$\mathbf{0.4701}$	< 0.0001	$\mathbf{0.1882}$	< 0.0001
r_V	$(0.1, 0.8)$	$\mathbf{0.8253}$	< 0.0001	$\mathbf{0.8065}$	< 0.0001	$\mathbf{0.6467}$	< 0.0001
b	$(10^3, 10^4)$	$\mathbf{-0.4944}$	< 0.0001	$\mathbf{-0.0675}$	< 0.0001	-0.0207	0.1439
g	$(0.1, 100)$	$\mathbf{0.0832}$	< 0.0001	0.0026	0.8570	-0.0201	0.1552
h	$(10^{-4}, 1)$	$\mathbf{0.0766}$	< 0.0001	0.0183	0.1967	0.0200	0.1581
δ_T	$(10^{-4}, 1)$	-0.0277	0.0502	-0.0154	0.2762	-0.0274	0.0534
M_C	$(0.01, 1)$	-0.0127	0.3704	-0.0055	0.6987	0.0162	0.2539
δ_C	$(10^{-4}, 1)$	-0.0108	0.4457	-0.0016	0.9109	-0.0015	0.9158
r_B	$(0.1, 0.8)$	-0.0067	0.6349	0.0116	0.4110	0.0052	0.7142
v_C	$(10^{-10}, 0.1)$	-0.0047	0.7425	-0.0163	0.2498	0.0039	0.7835
r_{Lt}	$(0.1, 0.8)$	0.0038	0.7864	$\mathbf{0.4869}$	< 0.0001	$\mathbf{0.7003}$	< 0.0001
M_T	$(0.01, 1)$	0.0032	0.8208	-0.0003	0.9815	0.0037	0.7955
r_{Ln}	$(0.1, 0.8)$	-0.0022	0.8751	-0.0003	0.9847	0.0209	0.1391
v_T	$(10^{-10}, 0.1)$	-0.0007	0.9629	-0.0150	0.2909	-0.0321	0.0235

the remaining mechanisms in an aggregate way using Lotka-Volterra equations as our main objective is to elucidate how bile acids influence colonization resistance against *C. difficile*.

The microbial interaction model suggests that *C. difficile* cannot colonize the gut in the presence of resident microbiota represented in the model by the Lachnospiraceae (L_n) and other bacteria (B). The steady state in which *C. difficile* vegetative cells (V) and Lactobacilliaceae (L_t) are absent and L_n and B co-exist is shown to be stable. For the post-antibiotic scenario, both groups (B and L_n) are necessary to suppress *C. difficile* colonization. Re-introducing either B or L_n alone is not sufficient to eliminate *C. difficile*. Therefore, perturbations that extensively reduce one or both bacterial populations can compromise colonization resistance.

These results align with the findings in both mouse and human studies looking at the interaction between the gut microbiota, antibiotics, and *C. difficile* infection (CDI). Prior to antibiotics the indigenous gut microbiota provides colonization resistance against *C. difficile* and it is not until perturbation by antibiotics that the microbial community allows for *C. difficile* colonization [32, 40]. The loss of gut bacterial diversity and members from the Lachnospiraceae and Ruminococcaceae families is associated with antibiotic use and *C. difficile* colonization [39]. Restoration of both is associated with resistance against *C. difficile* [39, 40]. Members of

the Lachnospiraceae family include many anaerobic Clostridia, which overlap in metabolic niche with *C. difficile*, potentially providing competition for nutrients in the gut after antibiotics. Mono-colonization with Lachnospiraceae strains in a germfree mouse ameliorated disease from CDI but did not eliminate *C. difficile* [16]. More recently, *C. scindens* and non-toxigenic *C. difficile*, both Clostridia, were able to decrease disease in an antibiotic treated CDI mouse model, although the precise mechanism is still unknown [7, 23]. There is also evidence of this in human studies, where a loss in bacterial diversity and members from the Lachnospiraceae and Ruminococcaceae families are associated with CDI [1, 35].

The analysis of the bile acid and combined models indicate that bile acids do not prevent *C. difficile* colonization, but they regulate the onset of *C. difficile* colonization and growth after antibiotic perturbation. This effect on the timing of colonization was particularly sensitive to DCA decay rate (δ_D) and the inhibition rate of *C. difficile* growth by DCA (b). In our models, the degradation of DCA was assumed to be first order kinetics, depending only on DCA concentration and δ_D was assumed constant and identical in both the pre- and post-antibiotic scenarios. It is plausible that DCA degradation dynamics are more complex. Model outcomes were also sensitive to the growth rate of *C. difficile* vegetative cells (r_V). Nevertheless, this opens up the possibility of somehow promoting DCA production to delay the onset of colonization and buy time for the pre-antibiotic microflora to be restored. We can test this experimentally in the future by treating antibiotic treated mice that are susceptible to *C. difficile* colonization with DCA orally. We can then challenge mice with *C. difficile* and define the level of colonization with and without the addition of DCA. We can also define the gut microbiota in these mice to measure the restoration of the gut microbiota after antibiotic treatment with and without the addition of DCA.

Similar to the combined model, it is evident that the production of secondary bile acids, such as DCA, by the gut microbiota is important for colonization resistance against *C. difficile*, reviewed here [47]. Secondary bile acids like DCA inhibit *C. difficile* growth *in vitro* and are also associated with resistance against *C. difficile* in mouse models [7, 36, 40]. More recently, patients with recurrent *C. difficile* that receive a fecal microbial transplant (FMT) show restoration of their fecal secondary bile acids, suggesting that microbial derived secondary bile acids could play an important role in the process of clearing CDI in humans as well [44]. However, the complex interactions between the microbiota, DCA and other bile acids in the gut need further investigation including studying kinetics, flux, and degradation dynamics over time in a gut that is healthy, antibiotic treated, and *C. difficile* colonized. Our model provides an early step in achieving this goal.

Our model can be expanded and refined in several ways. First, our model focuses on *C. difficile* colonization. However, once *C. difficile* reaches a high density in the gut, it produces toxins A and B, which cause gut damage. To address infection, the model should include the effects of toxins and the associated host response. Second, the effects of antibiotics on the gut microbiota were addressed in the model by modifying the initial conditions. Antibiotic perturbation in the gut microbiota could be included explicitly. Finally, microbial interactions were modeled using the Lotka-

Volterra equations, but nutrients and other interactions could be addressed in the model more explicitly by incorporating nutrient and other intermediate metabolites.

Acknowledgements The work was partially funded through the Research Collaborative Workshop for Women in the Mathematical Biology at the National Institute for Mathematical and Biological Synthesis, sponsored by the National Science Foundation through NSF Award DBI-1300426, with additional support from The University of Tennessee, Knoxville. Jabbari thanks the BBSRC and MRC for their support in the form of the grant awards BB/M021386/1 and G1002093. The work of Lanzas and Lenhart was partially supported by the joint NSF/NIGMS Mathematical Biology Program through NIH award R01GM113239. Theriot is funded by Career Development Award in Metabolomics grant K01GM109236 by NIH NIGMS.

References

[1] V.C. Antharam, E.C. Li, A. Ishmael, A. Sharma, V. Mai, K.H. Rand, and G.P. Wang. Intestinal dysbiosis and depletion of butyrogenic bacteria in *Clostridium difficile* infection and nosocomial diarrhea. *J. Clin. Microbiol.*, 51(9):2884–2892, 2013.

[2] L.C.M. Antunes, J. Han, R.B.R. Ferreira, P. Lolić, C.H. Borchers, and B.B. Finlay. Effect of antibiotic treatment on the intestinal metabolome. *Antimicrob. Agents Ch.*, 55(4):1494–1503, 2011.

[3] D. Artis. Epithelial-cell recognition of commensal bacteria and maintenance of immune homeostasis in the gut. *Nat. Rev. Immun.*, 8(6):411–420, 2008.

[4] M. Ballyk and H. Smith. A model of microbial growth in a plug flow reactor with wall attachment. *Math. Biosci.*, 158(2):95–126, 1999.

[5] C.M. Bassis, C.M. Theriot, and V.B. Young. Alteration of the murine gastrointestinal microbiota by tigecycline leads to increased susceptibility to *Clostridium difficile* infection. *Antimicrob. Agents Ch.*, 58(5):2767–2774, 2014.

[6] L. Bouillaut, W.T. Self, and A.L. Sonenshein. Proline-dependent regulation of *Clostridium difficile* Stickland metabolism. *J. Bacteriol.*, 195(4):844–854, 2013.

[7] C.G. Buffie, V. Bucci, R.R. Stein, P.T. McKenney, L. Ling, A. Gobourne, D. No, H. Liu, M. Kinnebrew, A. Viale, et al. Precision microbiome reconstitution restores bile acid mediated resistance to *Clostridium difficile*. *Nature*, 517(7533):205–208, 2015.

[8] M.E. Coleman, D.W. Dreesen, and R.G. Wiegert. A simulation of microbial competition in the human colonic ecosystem. *Appl. Environ. Microb.*, 62(10):3632–3639, 1996.

[9] R. Freter, H. Brickner, J. Fekete, M.M. Vickerman, and K.E. Carey. Survival and implantation of *Escherichia coli* in the intestinal tract. *Infect. Immun.*, 39(2):686–703, 1983.

[10] D.T. Grima, G.F. Webb, and E.M.C. D'Agata. Mathematical model of the impact of a nonantibiotic treatment for *Clostridium difficile* on the endemic

prevalence of vancomycin-resistant enterococci in a hospital setting. *Comp. Math. Meth. Med.*, 2012:1–8, 2012.

[11] I. Hall and E. O'Toole. Intestinal flora in new-born infants: with a description of a new pathogenic anaerobe, *Bacillus difficilis*. *Am. J. Dis. Child*, 49(2):390–402, 1935.

[12] S. Jabbari, S.T. Cartman, and J.R. King. Mathematical modelling reveals properties of TcdC required for it to be a negative regulator of toxin production in *Clostridium difficile. J. Math. Biol.*, 70:773–804, 2015.

[13] T. Karasawa, S. Ikoma, K. Yamakawa, and S. Nakamura. A defined growth medium for *Clostridium difficile*. *Microbiology*, 141(2):371–375, 1995.

[14] S. Karlsson, A. Lindberg, E. Norin, L.G. Burman, and T. Åkerlund. Toxins, butyric acid, and other short-chain fatty acids are coordinately expressed and down-regulated by cysteine in *Clostridium difficile*. *Infect. Immun.*, 68(10):5881–5888, 2000.

[15] Kirschner Lab - Publications: Uncertainty and Sensitivity Analysis. http://malthus.micro.med.umich.edu/lab/usanalysis.html, 2015.

[16] M.J. Koenigsknecht, C.M. Theriot, I.L. Bergin, C.A. Schumacher, P.D. Schloss, and V.B. Young. Dynamics and establishment of *Clostridium difficile* infection in the murine gastrointestinal tract. *Infect. Immun.*, 83(3):934–941, 2015.

[17] Cristina Lanzas, Erik R Dubberke, Zhao Lu, Kimberly Ann Reske, and YT Gröhn. Epidemiological model for *Clostridium difficile* transmission in healthcare settings. *Infection Control & Hospital Epidemiology*, 32(06):553–561, 2011.

[18] T.D. Lawley and A.W. Walker. Intestinal colonization resistance. *Immunology*, 138(1):1–11, 2013.

[19] M.P. Leatham, S. Banerjee, S.M. Autieri, R. Mercado-Lubo, T. Conway, and P.S. Cohen. Precolonized human commensal *Escherichia coli* strains serve as a barrier to *E. coli* O157: H7 growth in the streptomycin-treated mouse intestine. *Infect. Immun.*, 77(7):2876–2886, 2009.

[20] F.C. Lessa, Y. Mu, W.M. Bamberg, Z.G. Beldavs, G.K. Dumyati, J.R. Dunn, M.M. Farley, S.M. Holzbauer, J.I. Meek, E.C. Phipps, et al. Burden of *Clostridium difficile* infection in the United States. *New Engl. J. Med.*, 372(9):825–834, 2015.

[21] S. Marino, I.B. Hogue, C.J. Ray, and D.E. Kirschner. A methodology for performing global uncertainty and sensitivity analysis in systems biology. *J. Theor. Biol.*, 254(1):178–196, 2008.

[22] I.C. McKay and A. Speekenbrink. Implications of Freter's model of bacterial colonization. *Infect. Immun.*, 44(1):199–203, 1984.

[23] M.M. Merrigan, S.P. Sambol, S. Johnson, and D.N. Gerding. New approach to the management of *Clostridium difficile* infection: colonisation with non-toxigenic *C. difficile* during daily ampicillin or ceftriaxone administration. *Int. J. Antimicrob. Ag.*, 33:S46–S50, 2009.

[24] K.J. Nagaro, S.T. Phillips, A.K. Cheknis, S.P. Sambol, W.E. Zukowski, S. Johnson, and D.N. Gerding. Nontoxigenic *Clostridium difficile* protects

hamsters against challenge with historic and epidemic strains of toxigenic BI/NAP1/027 *C. difficile*. *Antimicrob. Agents Ch.*, 57(11):5266–5270, 2013.

[25] S. Nakamura, S. Nakashio, K. Yamakawa, N. Tanabe, and S. Nishida. Carbohydrate fermentation by *Clostridium difficile*. *Microbiol. Immunol.*, 26(2):107–111, 1982.

[26] S.J. O'Flaherty and T.R. Klaenhammer. Functional and phenotypic characterization of a protein from *Lactobacillus acidophilus* involved in cell morphology, stress tolerance and adherence to intestinal cells. *Microbiology*, 156(11):3360–3367, 2010.

[27] E.H. Otete, A.S. Ahankari, H. Jones, K.J. Bolton, C.W. Jordan, T.C. Boswell, M.H. Wilcox, N.M. Ferguson, C.R. Beck, and R.L. Puleston. Parameters for the mathematical modelling of *Clostridium difficile* acquisition and transmission: a systematic review. *PLoS One*, 8:e84224, 2013.

[28] R.C. Owens, C.J. Donskey, R.P. Gaynes, V.G. Loo, and C.A. Muto. Antimicrobial-associated risk factors for *Clostridium difficile* infection. *Clin. Infect. Dis.*, 46(Supplement 1):S19–S31, 2008.

[29] J. Pastor. *Mathematical ecology of populations and ecosystems*. Wiley-Blackwell, Singapore, 2011.

[30] J. Pépin, N. Saheb, M.-A. Coulombe, M.-E. Alary, M.-P. Corriveau, S. Authier, M. Leblanc, G. Rivard, M. Bettez, V. Primeau, et al. Emergence of fluoroquinolones as the predominant risk factor for *Clostridium difficile*–associated diarrhea: a cohort study during an epidemic in Quebec. *Clin. Infect. Dis.*, 41(9):1254–1260, 2005.

[31] M.C. Rea, C.S. Sit, E. Clayton, P.M. O'Connor, R.M. Whittal, J. Zheng, J.C. Vederas, R.P. Ross, and C. Hill. Thuricin CD, a posttranslationally modified bacteriocin with a narrow spectrum of activity against *Clostridium difficile*. *P. Natl. Acad. Sci.*, 107(20):9352–9357, 2010.

[32] A.E. Reeves, C.M. Theriot, I.L. Bergin, G.B. Huffnagle, P.D. Schloss, and V.B. Young. The interplay between microbiome dynamics and pathogen dynamics in a murine model of *Clostridium difficile* Infection. *Gut Microbes*, 2(3):145–158, 2011.

[33] J.M. Ridlon, D.-J. Kang, and P.B. Hylemon. Bile salt biotransformations by human intestinal bacteria. *J. Lipid Res.*, 47(2):241–259, 2006.

[34] J. Scaria, J.-W. Chen, N. Useh, H. He, S.P. McDonough, C. Mao, B. Sobral, and Y.-F. Chang. Comparative nutritional and chemical phenome of *Clostridium difficile* isolates determined using phenotype microarrays. *Int. J. Infect. Dis.*, 27:20–25, 2014.

[35] A.M. Schubert, M.A.M. Rogers, C. Ring, J. Mogle, J.P. Petrosino, V.B. Young, D.M. Aronoff, and P.D. Schloss. Microbiome data distinguish patients with *Clostridium difficile* infection and non-*C. difficile*-associated diarrhea from healthy controls. *MBio*, 5(3):e01021–14, 2014.

[36] J.A. Sorg and A.L. Sonenshein. Bile salts and glycine as cogerminants for *Clostridium difficile* spores. *J. Bacteriol.*, 190(7):2505–2512, 2008.

[37] R.R. Stein, V. Bucci, N.C. Toussaint, C.G. Buffie, Ratsch G., .G. Pamer, C. Sander, and J.B. Xavier. Ecological modeling from time-series inference:

insight into dynamics and stability of intestinal microbiota. *PLoS Comp. Biol.*, 9:e1003388, 2013.

[38] S.N. Steinway, M.B. Biggs, T.P. Loughran Jr, J.A. Papin, and R. Albert. Inference of network dynamics and metabolic interactions in the gut microbiome. *PLoS Comp. Biol.*, 11(6):e1004338, 2015.

[39] C.M. Theriot, A.A. Bowman, and V.B. Young. Antibiotic-induced alterations of the gut microbiota alter secondary bile acid production and allow for *Clostridium difficile* spore germination and outgrowth in the large intestine. *mSphere*, 1(1):e00045–15, 2016.

[40] C.M. Theriot, M.J. Koenigsknecht, P.E. Carlson Jr, G.E. Hatton, A.M. Nelson, B. Li, G.B. Huffnagle, J.Z. Li, and V.B. Young. Antibiotic-induced shifts in the mouse gut microbiome and metabolome increase susceptibility to *Clostridium difficile* infection. *Nat. Comm.*, 5, 2014.

[41] C.M. Theriot and V.B. Young. Interactions between the gastrointestinal microbiome and *Clostridium difficile*. *Annu. Rev. Microbiol.*, 69:445–461, 2015.

[42] M.C.B. Tsilimigras and A.A. Fodor. Compositional data analysis of the microbiome: fundamentals, tools, and challenges. *Ann. Epidemiol.*, 26(6):330–335, 2016.

[43] E.J. Vollaard and H.A. Clasener. Colonization resistance. *Antimicrob. Agents Ch.*, 38(3):409, 1994.

[44] A.R. Weingarden, C. Chen, A. Bobr, D. Yao, Y. Lu, V.M. Nelson, M.J. Sadowsky, and A. Khoruts. Microbiota transplantation restores normal fecal bile acid composition in recurrent *Clostridium difficile* infection. *Am. J. Physiol.-Gastr. L.*, 306(4):G310–G319, 2014.

[45] K.H. Wilson, M.J. Kennedy, and F.R. Fekety. Use of sodium taurocholate to enhance spore recovery on a medium selective for *Clostridium difficile*. *J. Clin. Microbiol.*, 15(3):443–446, 1982.

[46] K.H. Wilson and F. Perini. Role of competition for nutrients in suppression of *Clostridium difficile* by the colonic microflora. *Infect. Immun.*, 56(10):2610–2614, 1988.

[47] J.A. Winston and C.M. Theriot. Impact of microbial derived secondary bile acids on colonization resistance against *Clostridium difficile* in the gastrointestinal tract. *Anaerobe*, doi:10.1016/j.anaerobe.2016.05.003, 2016.